



저작자표시-비영리-변경금지 2.0 대한민국

이용자는 아래의 조건을 따르는 경우에 한하여 자유롭게

- 이 저작물을 복제, 배포, 전송, 전시, 공연 및 방송할 수 있습니다.

다음과 같은 조건을 따라야 합니다:



저작자표시. 귀하는 원저작자를 표시하여야 합니다.



비영리. 귀하는 이 저작물을 영리 목적으로 이용할 수 없습니다.



변경금지. 귀하는 이 저작물을 개작, 변형 또는 가공할 수 없습니다.

- 귀하는, 이 저작물의 재이용이나 배포의 경우, 이 저작물에 적용된 이용허락조건을 명확하게 나타내어야 합니다.
- 저작권자로부터 별도의 허가를 받으면 이러한 조건들은 적용되지 않습니다.

저작권법에 따른 이용자의 권리는 위의 내용에 의하여 영향을 받지 않습니다.

이것은 [이용허락규약\(Legal Code\)](#)을 이해하기 쉽게 요약한 것입니다.

[Disclaimer](#)

의학박사 학위논문

소라페닙과 DDC (Sodium diethyldithiocarbamate)
조합 요법으로 PI3K/Akt/mTOR 경로 억제를 통한 B
형 간염 유래 간암세포에서 세포자멸사를 유도함
에 대한 연구

**Combination of sorafenib and sodium
diethylthiocarbamate synergistically induce cell death
in hepatitis B virus derived liver cancer via
suppression of the PI3K/Akt/mTOR pathway**

울산대학교 대학원

의학과

권용재

Combination of sorafenib and sodium
diethylthiocarbamate synergistically induce
cell death in hepatitis B virus derived liver
cancer via suppression of the
PI3K/Akt/mTOR pathway

지도교수 남궁정만
탁은영

이 논문을 의학박사 학위 논문으로 제출함

2024년 8월

울산대학교 대학원
의학과
권용재

권용재 의학박사학위 논문을 인준함

심사위원	홍석경	(인)
심사위원	남궁정만	(인)
심사위원	탁은영	(인)
심사위원	이상훈	(인)
심사위원	윤영인	(인)

울 산 대 학 교 대 학 원

2024년 8월

Abstract

Background/Aims: This study explored the anti-cancer potential of combining sodium diethyldithiocarbamate (DDC), a disulfiram derivative, with sorafenib in HBV-positive liver cancer cells.

Methods: We assessed the expression levels of SOD1 and HBx using qRT-PCR and immunoblotting in liver cancer samples and cell lines. The PI3K/Akt/mTOR pathway was compared between HBV-positive and HBV-negative liver cancer cells. Cell viability, levels of reactive oxygen species, and apoptotic markers were examined in response to sorafenib and DDC combination treatment. Furthermore, we conducted an in vivo xenograft experiment involving oral gavage of sorafenib and DDC.

Results: Patient tissue samples and cells that were positive for HBV showed increased expressions of HBx and SOD1, with a significant correlation between the two. DDC treatment effectively reduced the expression of SOD1 and HBx in HepG2.2.15 cells. When combined, DDC and sorafenib synergistically decreased the expression of HBx. Sorafenib inhibited the PI3K/Akt/mTOR pathway in HBV-positive cells, and this inhibition was further enhanced by DDC, leading to decrease in cancer cell viability. However, the apoptotic markers did not show a significant increase. In an in vivo xenograft model, the combined oral administration of sorafenib and DDC synergistically inhibited tumor growth.

Conclusions: The combination of DDC and sorafenib effectively targets SOD1 and the PI3K/Akt/mTOR pathway in HBV-positive liver cancers. By reducing SOD1 expression, inducing oxidative stress, and suppressing cell viability, this combination therapy presents a promising strategy for the treatment of HBV-related liver cancers.

Index

Abstract	i
List of Figures	iii
Introduction	1
Materials and Methods	3
Results	7
Discussion	20
References	22
국문 요약	24

List of Figures

Figure 1. Basal expression of HBx and SOD1 in liver cancer cell lines and human tissue samples	8
Figure 2. Sorafenib sensitivity and PI3K/Akt/mTOR activation in liver cancer cell lines	11
Figure 3. Correlation between IC50 of sorafenib and PI3K/Akt/mTOR pathway activity, apoptosis-related markers, and protein expression of HBx and SOD1	12
Figure 4. Modulation of SOD1 expression in HepG2.2.15 cells with DDC of siSOD1 treatment	13
Figure 5. Impact of DDC on HepG2.2.15 cells with or without sorafenib treatment	15
Figure 6. Impact of DDC with or without sorafenib on cell death in HepG2.2.15 cells	17
Figure 7. Time-dependent changes in PI3K/Akt/mTOR pathway and Bcl-2/Bax levels in DDC, SF, and SF+DDC groups	18
Figure 8. Tumor xenograft mice treated with DDC with or without sorafenib	19

Introduction

Liver cancer is a major global health concern and is the sixth leading cause of cancer-related death worldwide [1]. Among the population of patients with chronic hepatitis B virus (HBV), liver cancer poses an even greater challenge [2], with an estimated 257 million individuals infected with HBV globally in 2018 [3]. HBV belongs to the Hepadnaviridae family and causes acute and chronic hepatitis by infecting the human liver. Despite the advancements in vaccine and therapeutic agents, current treatment strategies for HBV-infected patients primarily focus on reducing viral activity rather than achieving complete viral elimination. The difficulty arises from the persistence of integrated HBV DNA and transcriptionally inactive cccDNA [4]. Notably, a significant portion of the Korean population [5] and approximately 5% to 8% of the Chinese population [6] are affected by chronic HBV infections, which can potentially lead to the development of liver cancer, hepatitis, and cirrhosis, resulting in increased mortality rates [7].

HBV-related liver cancer is influenced by a complex interplay of viral and host factors [8]. Upon HBV infection, certain viral proteins such as HBx contribute to oncogenic processes characterized by dysregulated cell proliferation and evasive apoptosis mechanisms. Notably, the activation of the PI3K/Akt/mTOR pathway plays a significant role in promoting cell survival and growth in HBV-infected cells [9,10]. Chronic HBV infection leads to sustained inflammation, liver injury, and fibrosis, culminating in cirrhosis, a major risk factor for HCC [11]. Gaining a comprehensive understanding of these mechanisms, particularly the intricate involvement of the PI3K/Akt/mTOR pathway, is crucial for the development of effective prevention and treatment strategies targeting HBV-related liver cancer.

Sorafenib (brand name NexavarTM) is a standard therapy for liver cancer, including hepatocellular carcinoma (HCC). It acts by targeting multiple signaling pathways in tumor cells and blood vessels [12]. However, the development of sorafenib resistance in HBV-related liver tumors presents a major hurdle in achieving successful outcomes through standard therapy [13]. Therefore, finding effective treatment strategies for this subset of patients has become a critical area of research and clinical focus.

Recent studies have highlighted the potential of disulfiram (brand name AntabuseTM), an FDA-approved drug primarily used to treat alcohol addiction, in suppressing tumor growth and inhibiting viral replication [14,15]. Disulfiram has shown effectiveness against liver cancer and

has the potential to target cancer stem cells, presenting a novel approach to preventing tumor recurrence and metastasis [16]. Considering the promising results of disulfiram in different types of cancer, further research is needed to explore its role in liver cancer, especially in the context of HBV infection. The present study focuses on the combination of sorafenib and a disulfiram derivative, DDC, as a therapeutic regimen for the treatment of HBV-related liver cancer. The findings from this research have the potential to provide valuable insights into the treatment of this complex disease, leading to improved long-term survival rates.

Materials and methods

Patient tissue samples

Thirteen individual human liver cancer specimens were collected from patients who underwent hepatobiliary surgery at the Division of Liver Transplantation and Hepatobiliary Surgery in Asan Medical Center (Seoul, South Korea). Small fragments of the tumor were promptly frozen in liquid nitrogen and stored at -80°C until they were used for experimentation. The institutional Review Board (IRB) of Asan Medical Center reviewed and granted approval for the collection and utilization of patient specimens (approval no.2020-1464). All patients who provided tissue samples willingly donated their specimens and provided informed consent.

Cell culture

The HepG2.2.15 cell line was generously provided by Eui-Cheol Shin from Korea Advanced Institute of Science and Technology (KAIST, Daejeon, South Korea) [17]. HBV-negative liver cancer cell lines, including hepatoblastoma-derived HepG2 (ATCC No.HB-8065) [18], liver sinusoidal endothelial cell derived SK-HEP1 (ATCC No.HTB-52)[19], and adult hepatocellular carcinoma Huh-7 (KCLB No.60104), as well as the HBV-related liver cancer cell lines, pediatric hepatocellular carcinoma Hep3B (ATCC No.HB8064) and adult hepatocellular carcinoma SNU-449 (KCLB No.00449), were obtained from the Korean Cell Line Bank (KCLB; Korean Cell Line Research Foundation, Seoul, South Korea) or the American Type Culture Collection (ATCC; Manassas, VA, USA). All cell lines were cultured in DMEM with high glucose (Cat. No.SH30022.01; HyClone, Cytiva, Marlborough, MA, USA) for HepG2, HepG2.2.15, SK-HEP1,

and Hep3B or RPMI 1640 (Cat. No.SH30027.01; HyClone) for Huh-7 and SNU-449. The culture media were supplemented with 10% fetal bovine serum (FBA; Cat. No.F0600-050; GenDEPOT, Barker, TX, USA), 1% streptomycin/penicillin (Cat. No.SV30010.01; HyClone), and 0.2% Normocin (Cat. No.ANT-NR-2; InvivoGen, San Diego, CA, USA). The cells were maintained in an incubator at 37°C in a 5% CO₂ humidified environment.

Cell viability analysis

HepG2.2.15 cells were seeded in a 96-wall, flat-bottomed microplate (Cat. No.167008; Nunc, Thermo Fischer Scientific, Waltham, MA, USA) at a volume of 100 µl per well (0.8×10^5 cells/ml) and incubated overnight in a growth medium to facilitate cell adhesion. On the following day, the growth medium was replaced with fresh media, and the cells were treated with various concentrations of DDC alone and in combination with sorafenib (SF). The treated cells were then incubated for up to 24 h in a 5% CO₂ humidified environment at 37°C. After the incubation period, 10 µl of Cell Counting Kit-8 (CCK-8; CK04-13, Dojindo Laboratories, Kumamoto, Japan) solution was added to each well. Following a four-hour incubation in a 5% CO₂ humidified environment at 37°C, the cytotoxicity of the drugs was determined by measuring the absorbance at 450 nm using a Sunrise™ spectrophotometer (Tecan, Männedorf, Switzerland).

Immunoblotting assay

Protein expression was assessed using the Western blot technique. HepG2.2.15 cells were treated with DDC, sorafenib, or their combination for up to 24 h. To obtain the cell lysate, the cells were washed twice with DPBS and then extracted using RIPA buffer (50 mM Tris-HCl, pH 8.0, 1% NP-40, 0.5% sodium deoxycholate, 150 mM NaCl, and 0.1% sodium dodecyl sulfate) supplemented with a protease and phosphatase inhibitor cocktail (Cat. No. PPC1010; Sigma-Aldrich, Merck, Darmstadt, Germany). Human tissue samples were lysed in T-PER buffer (Cat. No.78510; Thermo Fisher Scientific) containing protease and phosphatase inhibitors. Protein extraction was carried out by centrifugation at $16,000 \times g$ for 15 min at 4°C. Protein concentrations were determined using the BCA Protein Assay Reagent (Cat. No.23225; Thermo Fisher Scientific). Equivalent amounts of protein from each sample were loaded onto polyacrylamide gels and separated through electrophoresis.

The separated proteins were then transferred to nitrocellulose membranes (Cat. No.1704270; Bio-Rad, Hercules, CA, USA). Blotting was performed using the TransBlot Turbo system (Bio-Rad) for 20 minutes. Subsequently, the membranes were blocked with 5% skim milk dissolved in Tris-buffered saline containing 0.1% Tween-20 (TBST) for 1 h at room temperature. After washing, the membranes were incubated overnight at 4°C with specific primary antibodies of interest, appropriately diluted with 5% BSA in TBST. Following primary antibody incubation, the membranes were probed with horseradish peroxidase-conjugated anti-mouse IgG or anti-rabbit IgG antibodies for 1 h at room temperature (Table 1).

Protein bands were developed using ECL SuperSignal™ West Femto Maximum Sensitivity Substrate (Cat. No.34095; Thermo Fisher Scientific, Waltham, MA, USA), and images were captured using the LuminoGraph II system (Cat. No.WSE-6200; ATTO, Tokyo, Japan).

RNA interference

Control and SOD1 siRNA were obtained from Bioneer (Daejeon, South Korea). HepG2.2.15 cells were seeded onto a 6-well plate and treated with siRNA using the Lipofectamine 2000 transfection system (Cat. No.11668-500; Invitrogen™, Thermo Fisher Scientific) following the product guidelines. To assess the efficacy of siRNA-mediated knockdown, we conducted a quantitative reverse transcription polymerase chain reaction (qRT-PCR) to quantify the mRNA levels of SOD1.

Total RNA Extraction and qRT-PCR

Total RNA was extracted from the cells using QIAzol reagent (Cat. No.79306; Qiagen, Germany), followed by phase separation using chloroform. The RNA samples were then purified using a silica column-based method (RNeasy Plus Mini Kit; Cat. No.74136; Qiagen). The concentration and purity of the extracted RNA were determined using the Nanodrop 2000 spectrophotometer. Subsequently, cDNA synthesis was performed using the ReverTra RT master mix (Cat. No.FSQ-301; Toyobo, Japan), facilitating the reverse transcription of RNA into complementary DNA (cDNA). The qRT-PCR analysis was conducted using the FIREPol EvaGreen qPCR Supermix (Cat. No.08-36-00001; Solis BioDyne, Tartu, Estonia) and the fluorescence intensity was quantified using the CFX Connect Real-Time PCR system (Cat.

No.1855201; Bio-Rad). To normalize the gene expression levels, the housekeeping gene *GAPDH* was employed as an internal control using the delta-delta Ct method.

Table 1. List of antibodies used for immunoblotting assay

Antibody name	Source	Catalog number and manufacturer	Dilution factor	Predicted size (kDa)
Superoxide Dismutase 1	Rabbit	ab16831, Abcam	1:1,000	17
Hep BxAg	Mouse	sc-57760, Santa Cruz Biotechnology	1:1,000	15
PI 3 Kinase catalytic subunit alpha (PIK3CA)	Rabbit	ab40776, Abcam	1:1,000	110
p-Akt1/2/3	Mouse	sc-514032, Santa Cruz Biotechnology	1:1,000	62/60/56
pan-AKT	Rabbit	ab8805, Abcam	1:1,000	56
p-mTOR	Mouse	sc-293133, Santa Cruz Biotechnology	1:1,000	220
mTOR antibody	Rabbit	ab2732, Abcam	1:1,000	289
Bcl2	Mouse	sc-7382, Santa Cruz Biotechnology	1:1,000	26
Bax	Mouse	sc-7480, Santa Cruz Biotechnology	1:1,000	23
4 Hydroxynonenal antibody (4-HNE)	Rabbit	ab46545, Abcam	1:1,000	72
PARP1 (Full)	Rabbit	ab32138, Abcam	1:1,000	113
PARP-1	Mouse	sc-74470, Santa Cruz Biotechnology	1:1,000	116/ 89/ 24
LC3B	Rabbit	ab51520, Abcam	1:1,000	16/18
β -Actin	Mouse	A3854, Sigma Aldrich	1:1,000	37

Reactive oxygen species measurement

To assess intracellular reactive oxygen species (ROS) generation in HepG2.2.15 cells following treatment, we used the H₂DCFDA cellular ROS assay kit from Abcam (Cat. No.ab113851; Abcam), following the manufacturer's instructions. The cells were treated with DDC, sorafenib, or their combination for 24 h in a 5% CO₂ humidified environment at 37°C.

After the treatment period, 20 μ M of H₂DCFDA in pre-incubated DPBS was added to the cells and incubated for 30 min. The relative intensities of green fluorescence in the different treatment groups were captured using the EVOS imaging system (Thermo Fisher Scientific). Fluorescence intensities were measured using ImageJ software (NIH, USA), and a histogram was prepared to compare the relative fluorescence intensities among the treatment groups.

Morphological assessment of apoptosis

To assess morphological changes indicative of apoptosis in HepG2.2.15 cells, we employed a microscopy-based approach utilizing the Annexin V-FITC kit (Cat. No. ab14085; Abcam). HepG2.2.15 cells were initially seeded in 6-well plates and incubated for 24 hours in a 5% CO₂ humidified environment at 37°C to facilitate cell adherence and growth. Following the incubation period, the cells were treated with DDC, sorafenib, or a combination of both for 24 hours. Subsequently, the treated cells were stained with Annexin V-FITC and Propidium Iodide (PI) to visualize apoptotic and dead cells. In addition to Annexin V, the cellular nucleus was stained using NucBlue™ Live Cell Stain (Cat. No. R37605; Thermo Fisher Scientific) following the manufacturer's instructions. The stained cells were then visualized using the EVOS system (Thermo Fisher Scientific).

Animal models

The NOD-*Rag2*^{-/-}*Il2rg*^{-/-} (NRG) immune-deficient mice (aged 7 - 8 weeks) were obtained from JA BIO (Gyeonggi-do, South Korea) for *in vivo* experiments. All animal procedures were approved by the Animal Research Committee of Asan Medical Institute for Life Sciences at Asan Medical Center (Seoul, South Korea) in accordance with the guidelines outlined in the Guide for Care and Use of Laboratory Animals (IACUC Approval No. 2019-13-071).

To evaluate the antitumor effect of DDC in combination with sorafenib, we injected HepG2.2.15 cells (1×10^6 cells/0.2 ml) into the liver parenchyma to establish liver orthotopic tumor xenografts. Mice were randomly divided into four groups (n = 8/group) and subjected to the following treatments: (a) vehicle control, (b) DDC (50 mg/kg/day, orally), (c) sorafenib (SF; 40 mg/kg/day, orally), or (d) DDC plus sorafenib (SF+DDC), administered for a duration of 3 weeks. At the end of the treatment period, the mice were euthanized in a humane manner, and liver tissues were

excised and processed for tumor regression analysis.

Statistical analysis

The data presented in this study are presented as the mean \pm standard deviation (SD). Statistical analysis was performed using one-way analysis of variance (ANOVA) with Bonferroni's post hoc analysis to assess differences between the individual treatment groups and the combination treatment group. A significance level of $P < 0.05$ was considered statistically significant.

Results

HBV-infected liver cancer cell lines and human specimens exhibit elevated SOD1 expression

In this study, we investigated the expression of SOD1 in HBV-infected liver cancer cell lines. The liver cancer cell lines HepG2.2.15, Hep3B, and SNU-449, which harbor integrated HBV genes, are known to express high levels of HBx protein, a key player in HBV infection. Additionally, we consistently observed increased expression of SOD1, a crucial antioxidant enzyme, at both the transcript and protein levels in HBV-infected liver cancer cells (**Figure 1A**). In HBV-positive liver cancer cells, the relative density of HBx protein (1.51 ± 0.38) was significantly higher than in HBV-negative cells (0.37 ± 0.08) ($P = 0.042$). SOD1 protein levels were also assessed, revealing higher expression in HBV-positive cells, although the difference between HBV-positive (2.09 ± 0.38) and HBV-negative (1.04 ± 0.05) cells did not reach the prespecified threshold for statistical significance ($P = 0.054$). Intriguingly, a strong positive correlation was observed between HBx and SOD1 expression ($R^2 = 0.97$, $p < 0.001$; **Figure 1B**). Our analysis also revealed that these HBV-infected cell lines exhibited significantly higher transcript levels of HBx and SOD1, compared to non-HBV expressing liver cancer-associated cell lines (**Figure 1C, D**).

Furthermore, our examination of liver cancer patients with HBV infection demonstrated a correlation between elevated HBx expression in liver tumor samples and tumoral SOD1 expression (**Figure 1E**). In liver tumor samples from non-HBV-patients, the expression of HBx was significantly lower (0.12 ± 0.04) compared to HBV-positive tumors (1.76 ± 0.23) ($P = 0.003$).

Similarly, the expression of SOD1 in non-HBV tumors (1.12 ± 0.19) was significantly lower than in HBV-positive tumors (4.04 ± 0.39) ($P = 0.002$). A correlation pattern similar to that observed in cell lines was also observed in patient tumor samples, with an even stronger correlation between HBx and SOD1 expression ($R^2 = 0.99$, $p < 0.001$; **Figure 1F**). Considering that HBV-positive liver cancers have previously been reported to exhibit resistance to sorafenib [13], the elevated levels of SOD1 observed in this study may provide a valuable clue in understanding the mechanisms underlying this resistance.

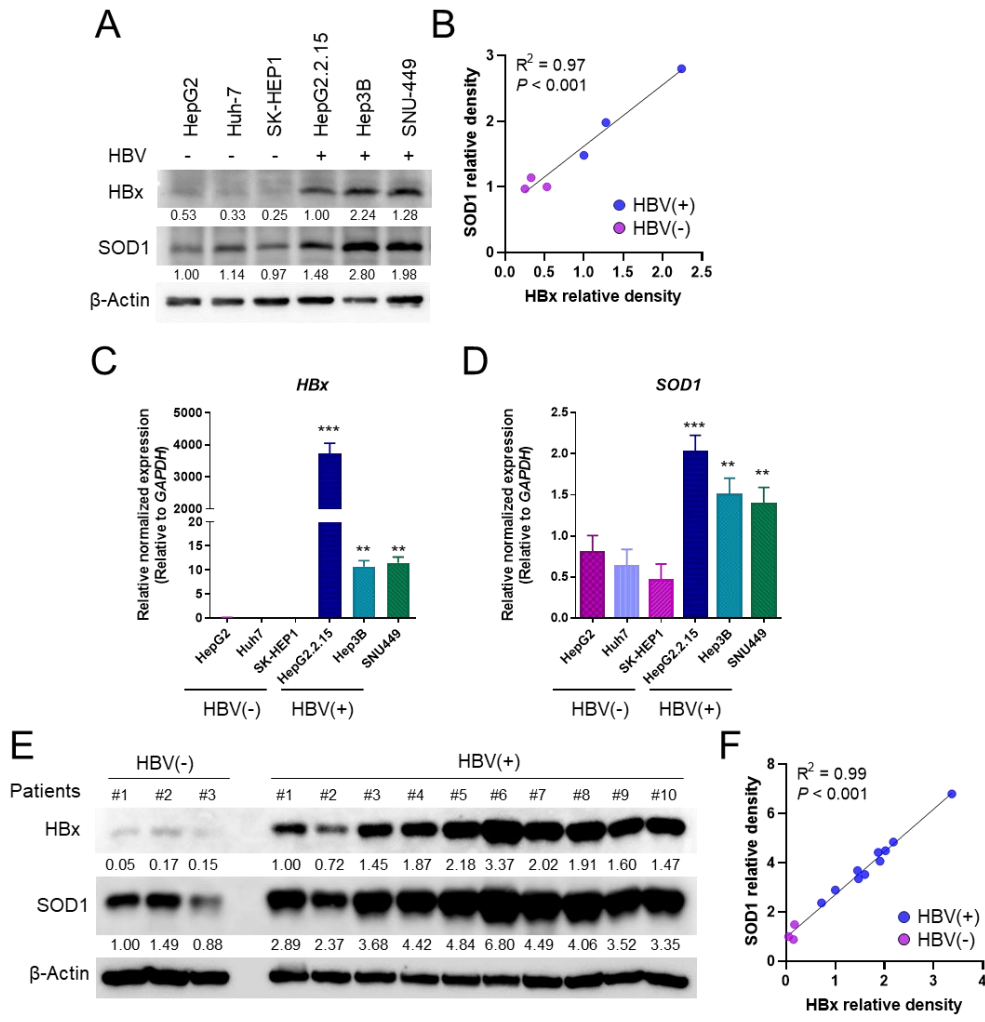


Figure 1. Basal expression of HBx and SOD1 in liver cancer cell lines and human tissue samples. (A) Basal expression levels of HBx and SOD1 proteins in HBV-negative liver cancer

cells (HepG2, Huh-7, SK-HEP1) and HBV-positive liver cancer cells (HepG2.2.15, Hep3B, SNU-449). **(B)** Correlation between the expression of HBx and SOD1 proteins ($P < 0.001$). **(C)** Expression of HBx and **(D)** SOD1 genes. **(E)** Human tissue proteins obtained from liver cancer patients categorized into HBV-negative and HBV-positive groups. The levels of HBx and SOD1 proteins were quantified. **(F)** Correlation between HBx and SOD1 protein expression in human liver cancer tissues ($P < 0.001$). Significance was determined using one-way ANOVA with Tukey's multiple comparisons test, with $P < 0.05$ considered significant.

Sorafenib response and PI3K/Akt/mTOR pathway activation in HBV-infected liver cancer cells

The effectiveness of sorafenib in treating liver cancer is dependent on the activation of the PI3K/Akt/mTOR pathway, which is a well-established contributor to drug resistance. Given that the HBx protein, which is commonly found in HBV-infected liver cells, can interact with the PI3K pathway, we investigated the interplay between sorafenib response and PI3K pathway activation in both HBV-negative and HBV-positive cells.

To evaluate the impact of HBV integration and HBx expression on cell death in response to sorafenib treatment, we measured the IC₅₀ values for HBV-negative and HBV-positive liver cancer cell lines (**Figure 2A**). Notably, the IC₅₀ value for HepG2.2.15 (IC₅₀ = 5.781) did not show a significant increase in sorafenib resistance when compared to HBx-negative HepG2 cells (IC₅₀ = 5.699). In contrast, HBx-positive Hep3B (IC₅₀ = 7.448) and SNU-449 (IC₅₀ = 7.896) cells exhibited higher IC₅₀ values, indicating greater resistance to sorafenib compared to HBV-negative SK-Hep1 (IC₅₀ = 4.306) and Huh-7 (IC₅₀ = 5.246) cells (**Figure 2C**).

Additionally, HBV-positive liver cancer cells showed elevated levels of key components in the PI3K/Akt/mTOR pathway including phosphorylated Akt (p-Akt) and Akt ratio (**Figure 2B and 2D**). Similarly, the levels of phosphorylated mTOR (p-mTOR) and the mTOR ratio were elevated in these cells (**Figure 2E**). Furthermore, the Bcl-2/Bax ratio, an indicator of anti-apoptotic status [20], was notably increased in HBV-infected cells (**Figure 2F**). While statistical significance was not reached for all parameters, it is worth noting that the levels of PI3K were higher in HBV-positive cells (4.89 ± 0.68) compared to HBV-negative cells (2.54 ± 0.79) ($P = 0.087$). Similarly, the p-Akt/Akt ratio was numerically higher in HBV-positive cells (2.71 ± 0.63)

compared to HBV-negative cells (1.46 ± 0.30) ($P = 0.148$). The p-mTOR/mTOR ratio was also numerically higher in HBV-positive cells (3.33 ± 0.49) compared to HBV-negative cells (1.03 ± 0.31) ($P = 0.124$). However the Bcl-2/Bax ratio was significantly higher in HBV-positive cells (1.82 ± 0.71) compared to HBV-negative cells (0.53 ± 0.24) ($P = 0.042$).

While not all parameters reached statistical significance, it is noteworthy that all HBV-containing cell lines exhibited indications of an activated PI3K/Akt/mTOR pathway and inhibited apoptosis-related mechanisms. These factors are well-established contributors to resistance against sorafenib. Moreover, our data revealed positive correlations between PI3K/Akt/mTOR activation and anti-apoptotic mechanisms with sorafenib IC₅₀ values (**Figure 3A-D**). Given the positive correlation between the IC₅₀ of sorafenib and the levels of HBx protein and SOD1 protein in liver cancer cell lines (**Figure 3E and 3F**), it can be assumed that cells with high HBx expression tend to exhibit elevated SOD1 levels and that both factors may be associated with sorafenib resistance.

Collectively, our findings suggest the activation of the PI3K/Akt/mTOR pathway and the inhibition of apoptosis-related mechanisms in HBV-positive liver cancer cells, which are known to contribute sorafenib resistance. In summary, the presence of HBV in liver cancer cells appears to enhance their resistance to sorafenib by activating the PI3K pathway and suppressing cell death mechanisms.

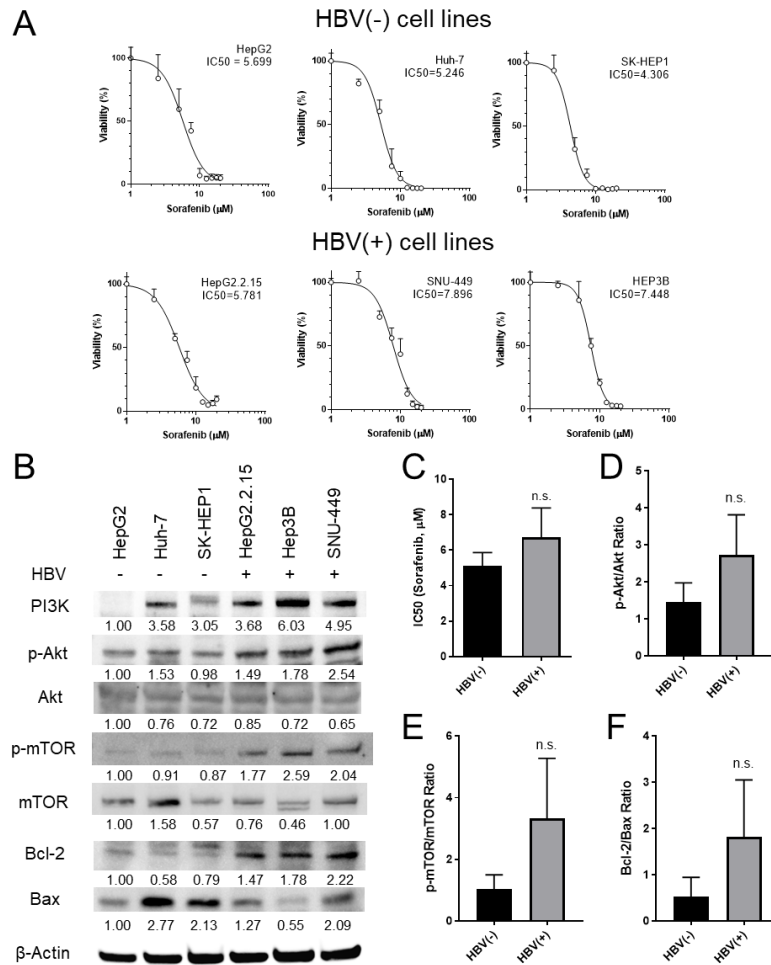


Figure 2. Sorafenib sensitivity and PI3K/Akt/mTOR activation in liver cancer cell lines. (A) WST-8 cell viability assay and IC₅₀ calculations in HBV-negative and HBV-positive liver cancer cell lines. Cells were treated with varying concentrations of sorafenib (0-20 µM) for 24hours. (B) Western blot analysis of PI3K/Akt/mTOR pathway activation and the Bcl-2/Bax ratio in HBV-negative and HBV-positive liver cancer cell lines. Relative protein densities are presented. (C) Average IC₅₀ values for HBV-negative and HBV-positive cells. (D) Average p-Akt/Akt ratio, (E) p-mTOR/mTOR ratio, and (F) Bcl-2/Bax ratio. Significance was determined using one-way ANOVA with Tukey's multiple comparisons test, with P < 0.05 considered significant

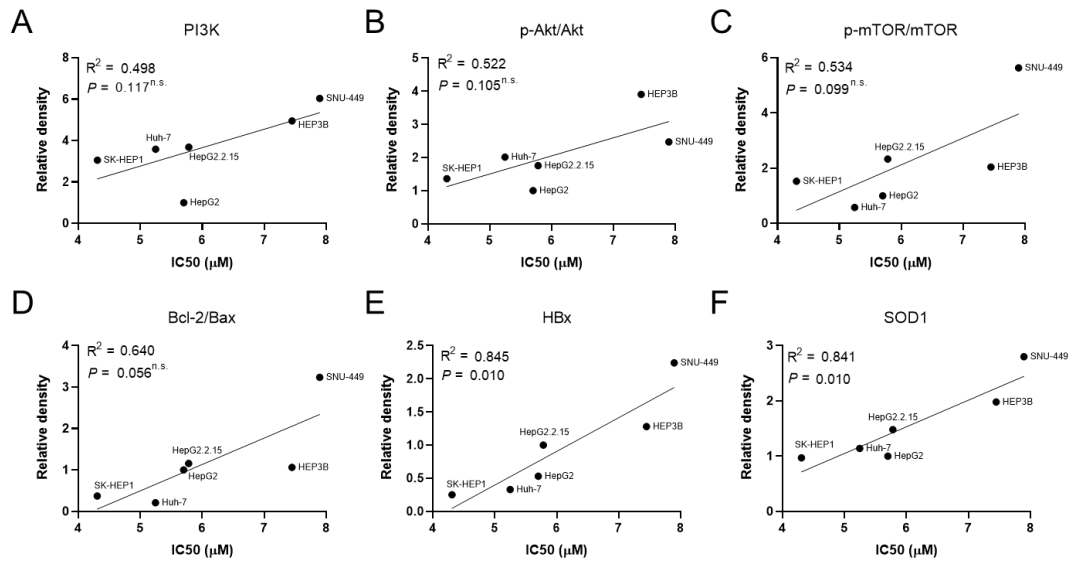


Figure 3. Correlation between IC50 of sorafenib and PI3K/Akt/mTOR pathway activity, apoptosis-related markers, and protein expression of HBx and SOD1. The correlation between IC50 (μM) of sorafenib and the protein levels of (A) PI3K, (B) pAkt/Akt, (C) p-mTOR/mTOR, (D) Bcl-2/Bax, (E) HBx, and (F) SOD1 measured in non-HBV (HepG2, SK-HEP1, Huh-7) or HBV-related liver cancer cell lines (HepG2.2.15, HEP3B, and SNU-449). A P value less than 0.05 was considered statistically significant.

SOD1 suppression enhances sorafenib-mediated cell death in HBV-infected liver cancer cells

Building upon our findings, we investigated the potential of DDC, a derivative of disulfiram known for its SOD inhibition properties, to reduce SOD1 expression in HepG2.2.15 cells. DDC treatment effectively suppressed SOD1 gene expression (**Figure 4A**). This intervention resulted in a significant decrease in the IC₅₀ of sorafenib (**Figure 4B**). Furthermore, to investigate the inhibition of SOD1 more comprehensively, we utilized siRNA-based suppression, which significantly increased sorafenib-induced cell death in HepG2.2.15 cells (**Figure 4C and 4D**).

In summary, our results highlight the potential of targeting SOD1 expression, either through DDC or siRNA-based suppression, to significantly enhance the effectiveness of sorafenib in inducing cancer cell death. This suggests a promising approach for adjunct therapy to enhance the effectiveness of sorafenib treatment.

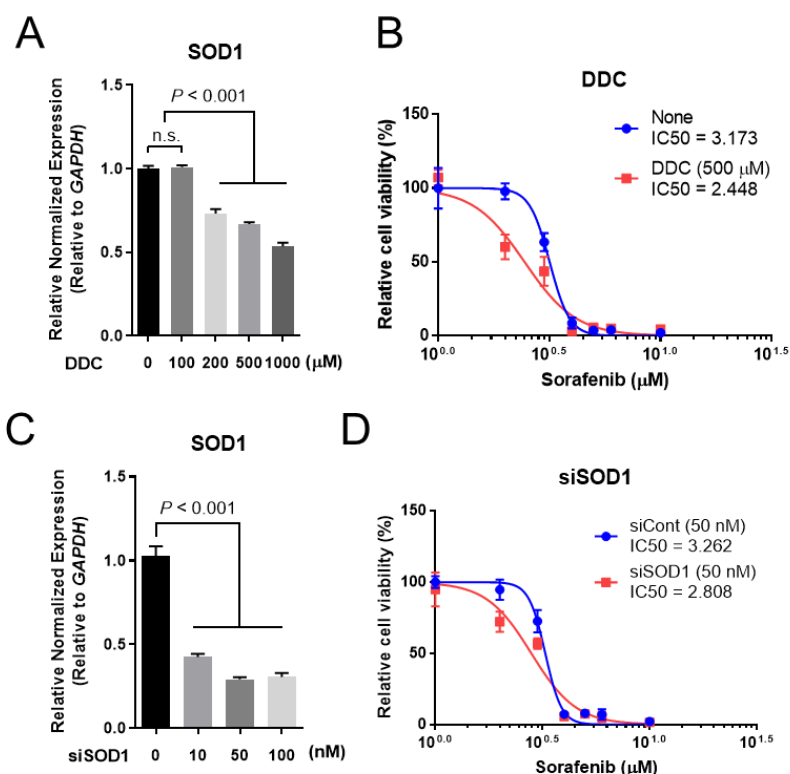


Figure 4. Modulation of SOD1 expression in HepG2.2.15 cells with DDC or siSOD1

treatment. (A-B) SOD1 expression in HepG2.2.15 cells following 24 h of DDC treatment **(A)** and the corresponding assessment of relative cell viability **(B)** at varying DDC concentrations. **(C-D)** SOD1 expression in HepG2.2.15 cells after 24 hours of siSOD1 treatment **(C)** and the corresponding evaluation of relative cell viability **(D)**. Significance was determined using one-way ANOVA with Tukey's multiple comparisons test, with $P < 0.05$ considered significant.

Synergistic effects of sorafenib and DDC on ROS accumulation

Based on our previous findings, which showed increased levels of SOD1 in HBV-positive HCC cell lines and the inhibitory effect of DDC on SOD1 expression, we aimed to examine whether the addition of DDC could enhance the effectiveness of sorafenib in inducing cell death in liver cancer. In our combined treatment approach, we observed a significant reduction in both HBx and SOD1 expression at both the mRNA and protein levels (**Figure 5A, B and C**).

Furthermore, we observed an increase in the expression of the lipid ROS marker, 4-hydroxynonenal (4-HNE), in the group receiving the combined treatment (**Figure 5C**). Our analysis using H₂DCFDA further revealed the highest ROS expression in the group treated with DDC in combination with sorafenib (**Figure 5D**). Although the area of FITC-positive cells showed an increase in all three experimental groups-DDC, sorafenib, and sorafenib + DDC, it is noteworthy that the sorafenib + DDC group displayed the highest fluorescent intensity (**Figure 5E**).

These findings strongly support our hypothesis that the combination of sorafenib and DDC synergistically inhibits HBx expression and leads to an accumulation of cellular ROS levels. Consistent with our previous data, which clearly demonstrated a strong correlation between cellular SOD1 expression and cellular HBx levels, the reduction in SOD1 may be intricately linked to HBx expression. However, it should be noted that while the inhibition of HBx can be associated with reduced SOD1 levels, the inhibition of SOD1 does not necessarily lead to the inhibition of HBx, as demonstrates in the case of sorafenib-alone treatment.

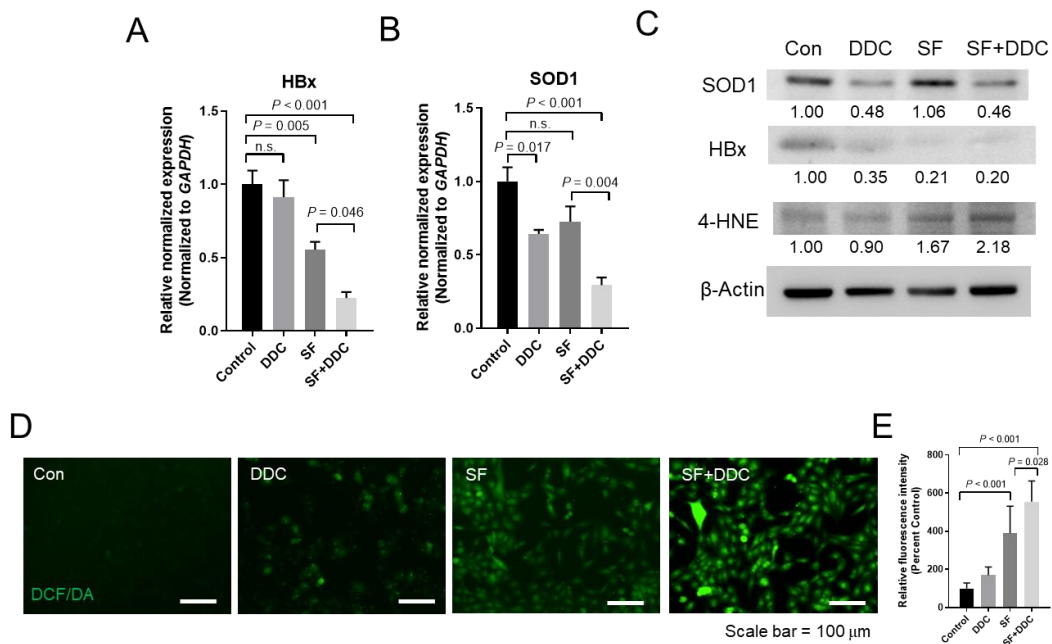


Figure 5. Impact of DDC on HepG2.2.15 cells with or without sorafenib treatment. (A-B) Gene expression levels of HBx (A) and SOD1 (B) in HepG2.2.15 cells treated with DDC with or without sorafenib. (C) Western blot analysis of SOD1, HBx, and 4-HNE in HepG2.2.15 cells treated with DDC with or without sorafenib, with relative protein densities presented. (D) Cellular ROS staining results using H2DCFDA assay in cells treated with DDC with or without sorafenib, and (E) quantification of relative fluorescence intensity. Significance was determined using one-way ANOVA with Tukey's multiple comparisons test, with $P < 0.05$ considered significant.

Combination of DDC and sorafenib increases cell death without augmenting apoptosis

We found a significant increase in cell death in HepG2.2.15 cells when treated with the combination of sorafenib and DDC. This prompted us to conduct further analysis to determine whether the increased cell death could be attributed to the ability of sorafenib to induce apoptosis in cancer cells. Interestingly, we did not observe an increase in cleaved PARP1 or cleaved Caspase-3, which are typical markers of apoptotic pathway activation (Figure 6A). Likewise, the autophagy marker LC3B remained unchanged in response to the combination therapy (Figure 6A). Upon further examination using Annexin V and PI fluorescence imaging, we observed an increase in cell death without a concurrent rise in cellular apoptosis (Figure 6B). Annexin V-FITC-

positive cells were most abundant under sorafenib-alone conditions (**Figure 6C**), while PI-positive cells peaked in the sorafenib + DDC combination treatment (**Figure 6D**). These results collectively indicate that the reduction in cell viability observed with sorafenib + DDC treatment is not primarily due to apoptotic cell death.

To gain insights into the underlying mechanisms, we conducted a comprehensive analysis of the activation of the PI3K/Akt/mTOR pathway (**Figure 6E**). Our results demonstrated that the combination treatment of sorafenib and DDC effectively inhibited the activation of this pathway. Notably, DDC treatment alone effectively suppressed SOD1 protein expression, while sorafenib alone had a slight stimulatory effect on SOD1 expression. Additionally, the presence of the HBx protein was strongly suppressed by the combined treatment (**Figure 6E**).

Markers associated with PI3K/Akt/mTOR pathway activation, including PI3K, the p-Akt/Akt ratio, and the p-mTOR/mTOR ratio, displayed a consistent upward trend over the course of drug treatment (up to 6hours), with the combined therapy exhibiting the most pronounced effects (**Figure 7A – 7C**). We also observed inhibition of both Bcl-2, an anti-apoptotic protein, and Bax, a pro-apoptotic protein, as a result of the combination therapy of DDC and sorafenib. Bcl-2 levels showed a slight increase when treated with sorafenib alone but were decreased by sorafenib + DDC. Bax protein also exhibited a slight increase in the sorafenib alone group and a decrease in sorafenib + DDC conditions. Nevertheless, the Bcl-2/Bax ratio, which indicates an anti-apoptotic response, consistently decreased in response to the sorafenib + DDC combined therapy (**Figure 7D**).

In conclusion, our findings suggest that the combination therapy of sorafenib and DDC enhances cell death in HepG2.2.15 cells through multiple mechanisms. This combination treatment effectively inhibits the expression of SOD1, which in turn affects the accumulation of intracellular ROS and inhibits the anti-apoptotic response of HBV-infected cells during sorafenib treatment. Moreover, it exerts significant effects on HBx protein levels and the activation of the PI3K/Akt/mTOR pathway, ultimately contributing to increase cell death.

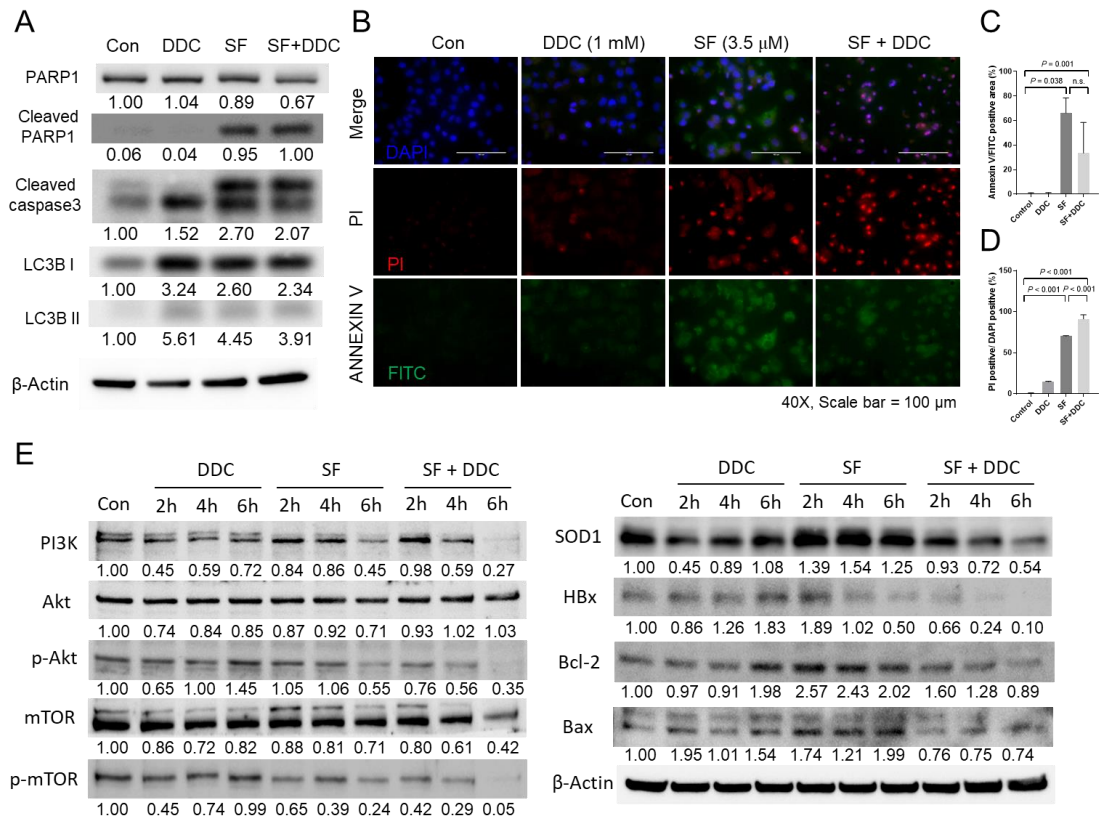


Figure 6. Impact of DDC with or without sorafenib on cell death in HepG2.2.15 cells. (A) Western blot analysis of apoptosis-related proteins (PARP1, cleaved PARP1, cleaved caspase3) and autophagy-related protein (LC3B) in HepG2.2.15 cells treated with DDC with or without sorafenib. **(B)** Fluorescence imaging analysis for apoptosis using Annexin V-FITC/PI staining in HepG2.2.15 cells subjected to DDC with or without sorafenib treatment. Quantification of **(C)** Annexin V-FITC positive area (%) and **(D)** PI-positive cells relative to DAPI-positive cells. **(E)** Evaluation of the PI3K/Akt/mTOR pathway and Bcl-2/Bax levels in cells treated with DDC, SF, or SF+DDC at various time points (2 h to 6 h). Significance was determined using one-way ANOVA with Tukey's multiple comparisons test, with $P < 0.05$ considered significant.

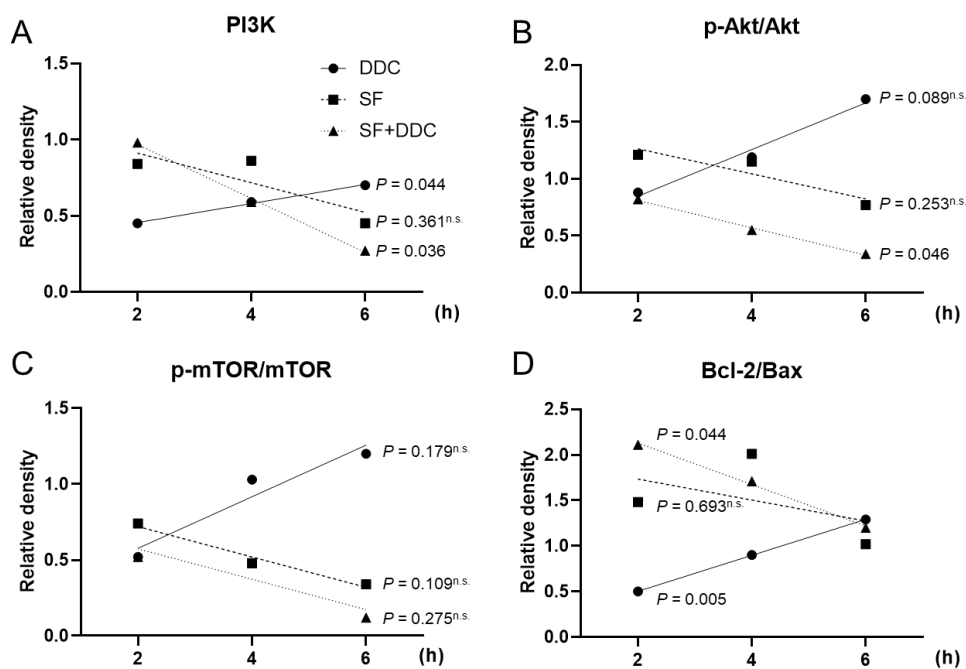


Figure 7. Time-dependent changes in PI3K/Akt/mTOR pathway and Bcl-2/Bax levels in DDC, SF, and SF+DDC groups. The correlation of (A) PI3K, (B) pAkt/Akt, (C) p-mTOR/mTOR, and (D) Bcl-2/Bax levels in HepG2.2.15 cells treated with DDC, sorafenib (SF), or the combination (SF+DDC) at different time points (2 h, 4 h, and 6 h). A P value less than 0.05 was considered statistically significant.

Combining sorafenib and DDC leads to tumor volume regression in orthotopic liver cancer xenograft mice

To evaluate the anticancer efficacy of combining DDC with sorafenib, we established an orthotopic liver cancer xenograft model using NRG mice and the HepG2.2.15 cell line. After allowing the implanted tumor cells to grow for 6 weeks, we randomly divided the mice into four groups, each consisting of 8 mice. Subsequently, the mice were treated with sorafenib (40mg/kg) or DDC (50mg/kg). Tumor samples were harvested on the 21st day of treatment (**Figure 8A**).

The results demonstrated that the combined treatment of sorafenib and DDC led to the most significant regression in tumor volume when compared to the other treatment groups (**Figure 8B and D**). Additionally, there was a significant decrease in body weight relative to their initial body

weight in mice treated with sorafenib alone or in combination with DDC (**Figure 8C**). Notably, the percentage of liver weight relative to the total body weight was lowest in the sorafenib + DDC group (**Figure 8D**).

Consistent with previous experimental findings indicating tumor regression, we observed a significant decrease in the expression of SOD1 in xenograft HepG2.2.15 tumors (**Figure 8E**). Both sorafenib and DDC significantly suppressed HBx expression in tumor tissues, with the sorafenib + DDC combined group showing the most effective reduction in HBx gene expression (**Figure 8F**). According to the previous *in vitro* experiment results, the *in vivo* xenograft animal model also revealed that liver tissue's SOD1 and HBx are decreased by DDC treatment. Furthermore, the combined treatment of DDC and sorafenib effectively inhibits SOD1 as well as HBx (**Figure 8G – I**). These results collectively highlight the role of DDC in reducing *in vivo* HBx-expressing liver cancer when administered in combination with sorafenib.

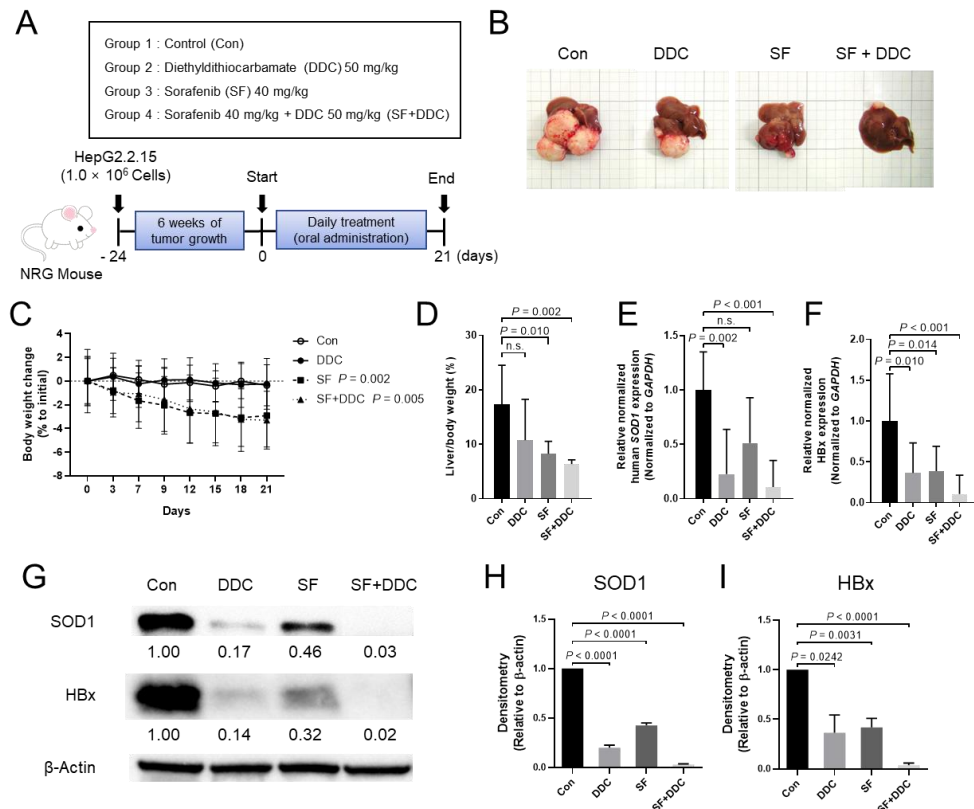


Figure 8. Tumor xenograft mice treated with DDC with or without sorafenib. (A) Schematic

diagram of the experiment. **(B)** Representative mice from each group: HCC control, sorafenib, DDC, and SF+DDC groups. **(C)** Percentage of body weight change relative to the initial weight. **(D)** Liver-to-body weight ratio (%). **(E)** SOD1 expression in each tumor. **(F)** HBx expression in each tumor. Significance was determined using one-way ANOVA with Tukey's multiple comparisons test, with $P < 0.05$ considered significant.

Discussion

In the context of global health challenge posed by liver diseases associated with HBV infection, the management of HBV-related liver cancer remains a significant clinical hurdle. HBV-related liver cancer is characterized not only by its role in promoting the proliferation of cancer cells but also by its resistance to apoptosis, making effective treatment a complex endeavor [21]. In this study, we explored the therapeutic potential of combining DDC with the traditional antineoplastic agent sorafenib to treat HBV-positive liver cancer.

The combination of DDC and sorafenib not only induced cell death through ROS-mediated programmed cell death but effectively inhibited the PI3K/Akt/mTOR signaling pathway. This observation suggests that the combined therapy has the potential to effectively inhibit the proliferation and survival of HBV-positive liver cancer cells. The PI3K/Akt/mTOR pathway is known to play a critical role in promoting cell growth, survival, and resistance to therapies [22]. The suppression of this pathway by the combined treatment of DDC and sorafenib provides a promising strategy to target specific vulnerabilities of HBV-positive liver cancer cells.

Also, the combined treatment of DDC and sorafenib has been shown to increase cellular levels of ROS, which can potentially lead to the inactivation of the PI3K pathway [23]. However, the specific type of cell death induced by this treatment remains unclear. Lipid ROS, such as 4-HNE, can modulate cellular signaling pathways, including the inhibition of the PI3K/Akt pathway [24]. The inactivation of the PI3K pathway can have diverse effects on cell fate, depending on the cellular context and other signaling pathways involved. Regarding the type of cell death observed in response to DDC and sorafenib treatment, it appears that the cell death mechanism is not solely apoptotic. Further investigation is needed to determine the specific type of cell death induced by DDC as well as the underlying mechanisms and pathways involved [25,26].

In conclusion, we found that combined treatment of DDC and sorafenib increased lipid ROS levels, potentially leading to the inactivation of the PI3K pathway. While our study provides important preliminary insights, further investigations are needed to fully elucidate the molecular mechanisms underlying this combination therapy and to explore its clinical applicability. The potential usefulness of the DDC and sorafenib combination therapy in the treatment of HBV-positive liver cancer warrants additional studies, including preclinical and clinical trials, to validate its efficacy and safety.

References

1. Villanueva A. Hepatocellular Carcinoma. *N Engl J Med* 2019;380:1450-62.
2. Yang JD, Hainaut P, Gores GJ, Amadou A, Plymoth A, Roberts LR. A global view of hepatocellular carcinoma: trends, risk, prevention and management. *Nat Rev Gastroenterol Hepatol* 2019;16:589-604.
3. Rehermann B, Thimme R. Insights From Antiviral Therapy Into Immune Responses to Hepatitis B and C Virus Infection. *Gastroenterology* 2019;156:369-83.
4. Naggie S, Lok AS. New Therapeutics for Hepatitis B: The Road to Cure. *Annu Rev Med* 2021;72:93-105.
5. Kim DY. History and future of hepatitis B virus control in South Korea. *Clin Mol Hepatol* 2021;27:620-2.
6. Wang H, Men P, Xiao Y, Gao P, Lv M, Yuan Q, et al. Hepatitis B infection in the general population of China: a systematic review and meta-analysis. *BMC Infect Dis* 2019;19:811.
7. Hsu YC, Huang DQ, Nguyen MH. Global burden of hepatitis B virus: current status, missed opportunities and a call for action. *Nat Rev Gastroenterol Hepatol* 2023;20:524-37.
8. Shoraka S, Hosseinian SM, Hasibi A, Ghaemi A, Mohebbi SR. The role of hepatitis B virus genome variations in HBV-related HCC: effects on host signaling pathways. *Front Microbiol* 2023;14:1213145.
9. Wang P, Guo QS, Wang ZW, Qian HX. HBx induces HepG-2 cells autophagy through PI3K/Akt-mTOR pathway. *Mol Cell Biochem* 2013;372:161-8.
10. Zhu M, Guo J, Li W, Xia H, Lu Y, Dong X, et al. HBx induced AFP receptor expressed to activate PI3K/AKT signal to promote expression of Src in liver cells and hepatoma cells. *BMC Cancer* 2015;15:362.
11. Michielsen PP, Francque SM, van Dongen JL. Viral hepatitis and hepatocellular carcinoma. *World J Surg Oncol* 2005;3:27.
12. Zhu YJ, Zheng B, Wang HY, Chen L. New knowledge of the mechanisms of sorafenib resistance in liver cancer. *Acta Pharmacol Sin* 2017;38:614-22.
13. Zhang S, Li N, Sheng Y, Chen W, Ma Q, Yu X, et al. Hepatitis B virus induces sorafenib resistance in liver cancer via upregulation of cIAP2 expression. *Infect Agent Cancer* 2021;16:20.
14. Chen HF, Hsueh PR, Liu YY, Chen Y, Chang SY, Wang WJ, et al. Disulfiram blocked cell entry of SARS-CoV-2 via inhibiting the interaction of spike protein and ACE2. *Am J Cancer Res* 2022;12:3333-46.
15. Xu L, Sun Y, Li Y, Sun J, Guo Y, Shen Q, et al. Disulfiram: A Food and Drug

- Administration-approved multifunctional role in synergistically drug delivery systems for tumor treatment. *Int J Pharm* 2022;626:122130.
16. Li Y, Wang LH, Zhang HT, Wang YT, Liu S, Zhou WL, et al. Disulfiram combined with copper inhibits metastasis and epithelial-mesenchymal transition in hepatocellular carcinoma through the NF-kappaB and TGF-beta pathways. *J Cell Mol Med* 2018;22:439-51.
 17. Sells MA, Chen ML, Acs G. Production of hepatitis B virus particles in Hep G2 cells transfected with cloned hepatitis B virus DNA. *Proc Natl Acad Sci U S A* 1987;84:1005-9.
 18. Lopez-Terrada D, Cheung SW, Finegold MJ, Knowles BB. Hep G2 is a hepatoblastoma-derived cell line. *Hum Pathol* 2009;40:1512-5.
 19. Tai Y, Gao JH, Zhao C, Tong H, Zheng SP, Huang ZY, et al. SK-Hep1: not hepatocellular carcinoma cells but a cell model for liver sinusoidal endothelial cells. *Int J Clin Exp Pathol* 2018;11:2931-8.
 20. Pepper C, Hoy T, Bentley DP. Bcl-2/Bax ratios in chronic lymphocytic leukaemia and their correlation with in vitro apoptosis and clinical resistance. *Br J Cancer* 1997;76:935-8.
 21. Zhang XD, Wang Y, Ye LH. Hepatitis B virus X protein accelerates the development of hepatoma. *Cancer Biol Med* 2014;11:182-90.
 22. Zhang H, Wang Q, Liu J, Cao H. Inhibition of the PI3K/Akt signaling pathway reverses sorafenib-derived chemo-resistance in hepatocellular carcinoma. *Oncol Lett* 2018;15:9377-84.
 23. Wen C, Wang H, Wu X, He L, Zhou Q, Wang F, et al. ROS-mediated inactivation of the PI3K/AKT pathway is involved in the antigastric cancer effects of thioredoxin reductase-1 inhibitor chaetocin. *Cell Death Dis* 2019;10:809.
 24. Ji GR, Yu NC, Xue X, Li ZG. 4-Hydroxy-2-nonenal induces apoptosis by inhibiting AKT signaling in human osteosarcoma cells. *ScientificWorldJournal* 2014;2014:873525.
 25. Solovieva M, Shatalin Y, Odinkova I, Krestinina O, Baburina Y, Mishukov A, et al. Disulfiram oxy-derivatives induce entosis or paraptosis-like death in breast cancer MCF-7 cells depending on the duration of treatment. *Biochim Biophys Acta Gen Subj* 2022;1866:130184.
 26. Wang L, Yu Y, Zhou C, Wan R, Li Y. Anticancer effects of disulfiram: a systematic review of in vitro, animal, and human studies. *Syst Rev* 2022;11:109.

국문 요약

목적: 본 연구는 디설피람 유도체인 DDC (sodium diethyldithiocarbamate)를 소라페닙과 조합하여 B형간염 유래 간암세포에서의 항암 작용 가능성을 확인하고자 하였다.

대상 및 방법: 간암 조직과 세포주에서 실시간 폴리머아제 연쇄반응(qRT-PCR)과 면역블롯팅(immunoblotting)을 사용하여 초과산화이온1 (SOD1)과 B형간염 바이러스 단백질(HBx)의 발현 수준을 확인하였다. B형간염 양성 간암세포와 B형간염 음성 간암세포에서 PI3K/Akt/mTOR 경로를 비교하였다. 소라페닙과 DDC 조합요법에서 세포 생존율, 활성산소 수준 및 세포자멸사 지표들을 평가했고, 소라페닙과 DDC의 경구 공급과 관련하여 이종이식 생체 내 실험을 수행하였다.

결과: 환자 조직 검체와 B형간염 양성 세포에서 HBx와 SOD1의 발현이 증가되어 있었으며 둘 사이에 유의한 상관관계가 있었다. DDC 치료는 HepG2.2.15 세포에서 SOD1과 HBx의 발현을 효과적으로 감소시켰다. DDC와 소라페닙의 조합요법은 HBx의 발현을 감소시켰다. 소라페닙은 B형간염 양성 세포에서 PI3K/Akt/mTOR 경로를 억제하였으며, 이는 DDC에 의해 더 강화되어 암세포 생존율을 감소시켰다. 그러나 세포자멸사 지표들의 유의한 증가를 보이지는 않았다. 이종이식 생체 내 실험에서 소라페닙과 DDC 조합요법의 경구 투약은 종양의 성장을 억제하였다.

결론: DDC와 소라페닙의 조합요법은 B형간염 유래 간암세포에서 SOD1과 PI3K/Akt/mTOR 경로에 효과적으로 작용한다. 이 조합요법은 SOD1의 발현을 감소시키고, 산화 스트레스를 유도하며, 세포 생존율을 억제함으로써 B형간염 유래 간암세포의 치료에 효과적인 전략이 될 수 있다.